Journal of Histochemistry & Cytochemistry 2017, Vol. 65(3) 125–138

DOI: 10.1369/0022155416687760
journals.sagepub.com/home/jhc
SAGE

Survival-Related Autophagic Activity Versus Procalcific Death in Cultured Aortic Valve Interstitial Cells Treated With Critical Normophosphatemic-Like Phosphate Concentrations

Antonella Bonetti, Alberto Della Mora, Magali Contin, Giorgia Gregoraci, Franco Tubaro, Maurizio Marchini, and Fulvia Ortolani

Departments of Experimental and Clinical Medicine (AB, ADM, MC, MM, FO), Medical and Biological Sciences (GG), and Agricultural, Food, Environmental and Animal Sciences (FT), University of Udine, Udine, Italy

Summary

Valve dystrophic calcification is a common disorder affecting normophosphatemic subjects. Here, cultured aortic valve interstitial cells (AVICs) were treated 3 to 28 days with phosphate (Pi) concentrations spanning the normal range in humans (0.8, 1.3, and 2.0 mM) alone or supplemented with proinflammatory stimuli to assess possible priming of dystrophic-like calcification. Compared with controls, spectrophotometric analyses revealed marked increases in calcium amounts and alkaline phosphatase activity for 2.0-mM-Pi-containing cultures, with enhancing by proinflammatory mediators. Ultrastructurally, AVICs treated with low/middle Pi concentrations showed an enormous endoplasmic reticulum (ER) enclosing organelle debris, so apparently executing a survival-related atypical macroautophagocytosis, consistently with ultracytochemical demonstration of ER-associated acid phosphatase activity and decreases in autophagosomes and immunodetectable MAP1LC3. In contrast, AVICs cultured at 2.0-mM Pi underwent mineralization due to intracellular release and peripheral layering of phospholipid-rich material acting as hydroxyapatite nucleator, as revealed by Cuprolinic Blue and von Kossa ultracytochemical reactions. Lack of immunoblotted caspase-3 cleaved form indicated apoptosis absence for all cultures. In conclusion, fates of cultured AVICs were crucially driven by Pi concentration, suggesting that serum Pi levels just below the upper limit of normophosphatemia in humans may represent a critical watershed between macroautophagy-associated cell restoring and procalcific cell death. (J Histochem Cytochem 65:125–138, 2017)

Keywords

aortic valve interstitial cells, autophagy, calcific valve disease, ectopic calcification, electron microscopy, phosphatemia

Introduction

In developed countries, heart valve dystrophic calcification is a common disorder affecting normophosphatemic subjects.[1] Normal serum phosphate (Pi) levels conventionally range from a minimum of 0.8 to 1.45 mM[2,3] to a maximum of 2.0 to 2.1 mM,[4,5] which

Received for publication October 6, 2016; accepted December 13, 2016.

Corresponding Author:
Fulvia Ortolani, Department of Experimental and Clinical Medicine, University of Udine, Piazzale M. Kolbe 3, I-33100 Udine, Italy.
E-mail: fulvia.ortolani@uniud.it

Journal of Histochemistry & Cytochemistry

represent threshold values for proper functioning of cellular and systemic processes. Several cohort studies indicated high serum Pi levels within the normophosphatemic range to be associated with increased risk of cardiovascular diseases, including ectopic calcification.[2,3,6–8] Actually, elevated Pi concentrations act as critical biomineralization determinants,[4,9,10] triggering the precipitation of hydroxyapatite (HA) crystals in diseased tissues. Besides depending on Pi concentration, it is widely accepted that cardiovascular tissue calcification also correlates with active processes, including accumulation and/or alteration of lipids, inflammation, loss of anticalcific proteins, cell osteogenic differentiation, and cell death.[11–16] In particular, apoptosis- and macroautophagocytosis-derived bodies are reported as HA-nucleating structures, playing a procalcific role as matrix vesicles do in mineralizing cartilage and bone.[17–21] Using original in vitro models simulating either severe dystrophic calcification[22] or metastatic calcification,[23] aortic valve interstitial cell (AVIC) mineralization resulted to be triggered by elevated Pi alone and enhanced after superstimulation with lipopolysaccharide (LPS) and proinflammatory mediators derived from cultures of LPS-stimulated macrophages. The induced calcific process depended on a distinct cell degeneration involving membrane colliquation, lipid release, and formation of peripheral phthalocyanine-positive layers (PPLs) at the level of dying cells and derived cell debris, acting as major HA nucleators. Comparable features were previously reported for both in vivo experimentally induced aortic valve mineralization[24–27] and actual ectopic calcification.[11,28–30] In the present study, similar in vitro models were used to simulate different normophosphatemic-like conditions by treating AVICs with Pi concentrations spanning the normal range in humans and including the borderline ones, with or without superstimulation with proinflammatory mediators. AVICs treated with low/middle Pi concentrations were found to undergo atypical autophagy preserving cells from death and subsequent mineralization. In contrast, AVICs exposed to the highest Pi concentration underwent prominent non-apoptotic, lipid-release-associated procalcific cell degeneration and death, supporting the concept that concentration-dependent procalcific effects in organisms may be exerted by Pi at the most elevated levels even within the normal range.

Materials and Methods

AVIC Isolation

Tricuspid aortic roots were excised from hearts (n=3) of healthy bovines slaughtered in a local abattoir (Salumificio Pitaccolo G. Srl - Macellazione & sezionamento carni; Castions di Strada, Udine, Italy), in which the rules of Reg CE 1099/2009, September 24, 2009, concerning the protection of animals at the time of killing were respected. Cows were not killed specifically for the purpose of the present study, and no experiments were performed on animals before slaughtering. Aortic roots were placed in cooled DMEM (Sigma, St. Louis, MO) supplemented with 1% penicillin/streptomycin and 1 µg/ml amphotericin B. Once isolated from aortic roots and subjected to removal of samples destined to microscopic examination, all valve leaflets underwent AVIC extraction procedure. Cell extraction and subsequent in vitro treatments were performed separately for each aortic root to avoid pooling of AVICs from different animals. For AVIC extraction, aortic leaflets were (1) depleted of endothelial cells by gentle scraping, (2) minced into about 2- to 3-mm^3 pieces, and (3) enzymatically digested with type I collagenase (125 U/ml; Sigma), elastase (8 U/ml; Sigma), and soybean trypsin inhibitor (0.375 mg/ml; Sigma) for 30 min at 37C in a CO_2 incubator. Then, digested pieces were transferred into 100-mm tissue culture Petri dishes (Greiner Bio-One, Frickenhausen, Germany) and cultured in DMEM supplemented with 20% FBS (Gibco–Invitrogen, Carlsbad, CA), 1% L-glutamine, and 1% penicillin/streptomycin. After 7 to 10 days, digested pieces were removed and drawn AVICs were cultured in complete DMEM as above, refreshing the culture medium every 3 days. At confluence, AVICs were expanded up to 12 folds. For experimental trials, cells from passage 4 were used.

Conditioned Medium (CM) From Bovine Macrophages

Peripheral blood was drawn from healthy bovines (n=2) during routine care. Blood was collected by the veterinarian in the whole respect of animal normal behavior and wellness, according to both Italian legislation (D.L. No. 116, January 27, 1992), in line with European Economic Community (EEC) regulation No. 86/609, November 24, 1986, and the professional ethics of Italian veterinarians (Federazione Nazionale Ordini Veterinari Italiani [FNOVI], June 12, 2011). Blood cell separation was performed separately for each animal. Namely, blood was diluted 1:2 with PBS solution and subjected to Ficoll (Sigma) density gradient centrifugation. Collected lymphocytes and monocytes were plated on tissue culture flasks and maintained in DMEM supplemented with 10% FBS, 1% L-glutamine, and 1% penicillin/streptomycin overnight. After lymphocyte removing, monocytes were cultured in complete DMEM

for 3 days to promote cell differentiation. Macrophages were then stimulated with 100 ng/ml LPS (Sigma) for 1 hr at 37C, rinsed twice with DMEM plus 10% FBS, and cultured in complete DMEM for 12 hr to allow cell degranulation. After culture medium collection and centrifugation, supernatants were 0.22-µm-filtered, supplemented with 1% polymyxin B (Sigma) to neutralize residual LPS, and stored at –20C until use.

Cell Culture Treatments

At preconfluence, cultured AVICs were treated for 3, 9, 15, 21, 25, and 28 days with (1) DMEM supplemented with 10% FBS, 1% L-glutamine, and 1% penicillin/streptomycin (control-cultures) or culture medium as in (1) supplemented with different volumes of 0.5-M sodium dihydrogen phosphate solution to obtain final concentrations equal to (2) 0.8-mM Pi (0.8-Pi-cultures), (3) 1.3-mM Pi (1.3-Pi-cultures), and (4) 2.0-mM Pi (2.0-Pi-cultures) or culture media as in (2), (3), and (4) supplemented with 100 ng/ml LPS and 20% (v/v) bovine macrophage CM (0.8-Pi-LPS-CM-cultures, 1.3-Pi-LPS-CM-cultures, and 2.0-Pi-LPS-CM-cultures, respectively). Parallel 2.0-Pi-LPS-CM-cultures were treated with a prevalidated concentration of 20-µM pancaspase inhibitor Boc-D-FMK (Sigma) for 28 days. Both culture and stimulating media were renewed every 3 days. All experiments were performed in triplicates.

Spectrophotometric Quantification of Calcium Content

After culture medium recovering, AVICs were scraped, centrifuged, and treated with a lysis buffer containing 50-mM TRIS-HCl, 150-mM NaCl, 5-mM EDTA, and 1% Triton X-100, pH 7.4, for 1 hr at 4C. After microcentrifugation at 2000 rpm for 5 min, part of supernatants (500 µL) was recovered for protein assay, whereas the remaining volumes were added to their original culture media and transferred into distinct Teflon vessels containing 1 ml of 65% suprapure grade nitric acid (Merck Millipore, Darmstadt, Germany) and 500 µL of 30% suprapure hydrogen peroxide (Merck Millipore). Then, samples were irradiated at 250 W for 2 min, 0 W for 2 min, 300 W for 5 min, 450 W for 5 min, and 650 W for 6 min using the Milestone High Performance Microwave Digestion Unit MLS 1200 Mega (Shelton, CT). After dilution with ultrapure water up to 100 ml of total solution, calcium quantification was assessed using the o-cresolphthalein complexone method (Chema Diagnostica, Monsano, Italy) reading the absorbance at 575 nm with the Varian Cary 50 Bio Spectrophotometer (Midland, Ontario, Canada). The estimated values were the mean of 10 readings of each three-times repeated culture (*n*=3), which were normalized on the basis of total protein content.

Spectrophotometric Quantification of Protein Content and Alkaline Phosphatase Activity

Supernatants obtained from lysed samples as described above were used to quantify both total protein content and alkaline phosphatase (ALP) activity. Total protein content was estimated using the Pierce Coomassie (Bradford) Protein Assay kit (Thermo Fisher Scientific, Waltham, MA) reading the absorbance at 595 nm using the aforementioned Varian spectrophotometer. ALP activity was assayed using a kinetic method based on measurement of 4-nitrophenol production (Chema Diagnostica) with absorbance reading at 405 nm, at 37C, within the first 5 min of enzymatic activity using the Varian spectrophotometer as above. Values were obtained by calculating the trend line gradients resulting from the mean of three readings of each three-times repeated culture (*n*=3), which were normalized on the basis of total protein content.

Alizarin Red S Calcium Staining

After culture medium removal, AVIC monolayers were rinsed with Pi buffer and fixed with neutral-buffered 5% formalin for 10 min. After further rinsing, AVIC monolayers were incubated in an aqueous solution of 2% alizarin red S (CARLO ERBA Reagents, Milano, Italy), pH 4.2, for 5 min; rinsed again to remove exceeding staining solution; and covered with distilled water. As negative controls, parallel AVIC monolayers were treated with a decalcifying solution containing 0.05-M sodium acetate buffer and 0.05-M magnesium chloride, pH 4.8, for 1 hr before alizarin red S staining. Observations and photographic records were made using the Olympus IX70 inverted microscope (Hicksville, NY).

Preembedding Cuprolinic Blue Reaction for Ultrastructural Polyanion Evidentiation

After culture medium removal, AVIC monolayers were incubated in 25-mM sodium acetate buffer, pH 4.8, containing 0.05% phthalocyanine Cuprolinic Blue (CB; Electron Microscopy Sciences, Hatfield, PA), 0.05-M magnesium chloride, and 2.5% glutaraldehyde overnight at room temperature keeping culture plates under continuous agitation. After washing, AVIC monolayers were postfixed with phosphate-buffered 2% osmium tetraoxide (Agar Scientific, Stansted, UK) for 1 hr at 4C, washed again, dehydrated in graded ethanols, and embedded in Epon 812 resin. Ultrathin sections were

collected on formvar-coated 2 × 1-mm-slot copper grids and contrasted with uranyl acetate and lead citrate. Observations and photographic recordings were made using the Philips CM12 STEM electron microscope (Eindhoven, The Netherlands).

Postembedding von Kossa Silver Staining for Ultrastructural Calcium-Binding Site Evidentiation

Semithin sections of CB-reacted AVIC monolayers were mounted on glass slides, covered with a drop of 1% silver nitrate solution, and placed on an 80C warm plate for 15 min under direct sunlight. After washing with distilled water and drying, semithin sections were covered with a drop of 5% sodium thiosulfate reducing solution and warmed at 80C for 5 min. After further washing and drying, reacted semithin sections were reembedded by gluing onto the slides top-less conic BEEM capsules (Agar Scientific, Stansted, UK), so encircling each semithin section, which were filled with Epon-Araldite fluid. After resin polymerization, reembedded sections were detached from slides and cut to obtain ultrathin sections which were collected, contrasted, observed, and recorded as above.

Ultrastructural Localization of Acid Phosphatase Activity

After culture medium removal, AVIC monolayers were fixed with 3% paraformaldehyde for 30 min, washed with 0.05-M sodium acetate buffer, pH 5.0, and incubated in the same buffer supplemented with 0.01-M beta-glycerophosphate (Sigma) and 0.004-M lead nitrate for 45 min at 37C. As negative controls, incubating solutions lacking in beta-glycerophosphate were used. After washing with cooled 0.05-M sodium acetate buffer to block enzymatic activity, AVIC monolayers were (1) fixed with 2% glutaraldehyde for 15 min, (2) postfixed with 2% osmium tetraoxide for 1 hr at 4C, (3) dehydrated in graded ethanols, and (4) embedded in Epon 812 resin. Ultrathin sections were collected, contrasted, observed, and recorded as above.

Immunocytochemistry

Monolayers of AVICs seeded on 24 × 24-mm coverslips placed at the bottom of 35-mm culture plates were incubated in (1) 0.1% Triton X-100 solution for 10 min, (2) 3% hydrogen peroxide solution for 5 min, (3) 3% normal serum solution for 30 min, (4) 1:600 rabbit anti-MAP1LC3 polyclonal antibody (Merck Millipore) or 1:25 goat anti-annexin-V polyclonal antibody (Santa Cruz Biotechnology, Santa Cruz, CA) for 2 hr at room temperature in a humidified chamber, and (5) 1:600 anti-rabbit peroxidase-conjugated secondary antibody (Jackson ImmunoResearch, West Grove, PA) or 1:400 anti-goat peroxidase-conjugated secondary antibody (Santa Cruz Biotechnology) for 30 min at room temperature. As negative controls, primary antibodies were replaced by normal serum. Peroxidase activity was revealed incubating AVIC monolayers in a solution containing diaminobenzidine tetrahydrochloride (DAB) and hydrogen peroxide (BioGenex, San Ramon, CA) for 3 to 6 min. After rinsing with distilled water to block enzymatic activity, cells were weakly counterstained with hematoxylin. Coverslips were then mounted on glass slides using an aqueous mounting medium, observed, and recorded using a Zeiss Axio Imager photomicroscope (Jena, Germany). Percentage values of immunopositive cells were estimated using the ImageJ software, averaging the number of reactive cells in five distinct areas of each three-times repeated AVIC culture (n=3).

Western Blotting

AVIC cultures were subjected to cell lysis and protein quantification as described above. Supernatants were then separated by SDS-PAGE and transferred on nitrocellulose membranes by electroblotting using the Bio-Rad Mini Trans-Blot system (Hercules, CA). After blocking with 3% skim milk (Sigma) solution, blotted membranes were incubated with 1:500 rabbit anti-cleaved-caspase-3 polyclonal antibody (Cell Signaling Technology, Danvers, MA) overnight at 4C and then with 1:15,000 anti-rabbit peroxidase-conjugated secondary antibody (Sigma) for 1 hr at room temperature. Immunoreactive bands were revealed using the Pierce enhanced chemiluminescence assay (Thermo Fisher Scientific) with a maximum exposure time of 4 hr. For accurate estimation of protein molecular weight, Precision Plus Protein Standards (Bio-Rad) were used. As positive controls, lysates of AVICs treated with 50-µM etoposide (Sigma) for 18 hr were used.

Statistical Analysis

Continuous variables were summarized as mean ± standard deviation. Data were tested for normal distribution using the Shapiro–Wilk test. Equality of variance was assessed using the Levene test. The variation of calcium amounts or ALP activity between groups (control, Pi, and Pi-LPS-CM) throughout incubation times was explored using the linear mixed models for longitudinal data. Comparisons between the three groups for each incubation time were performed using the ANOVA test or Kruskal–Wallis test, as appropriate. Comparisons between two groups were performed using the t-test or

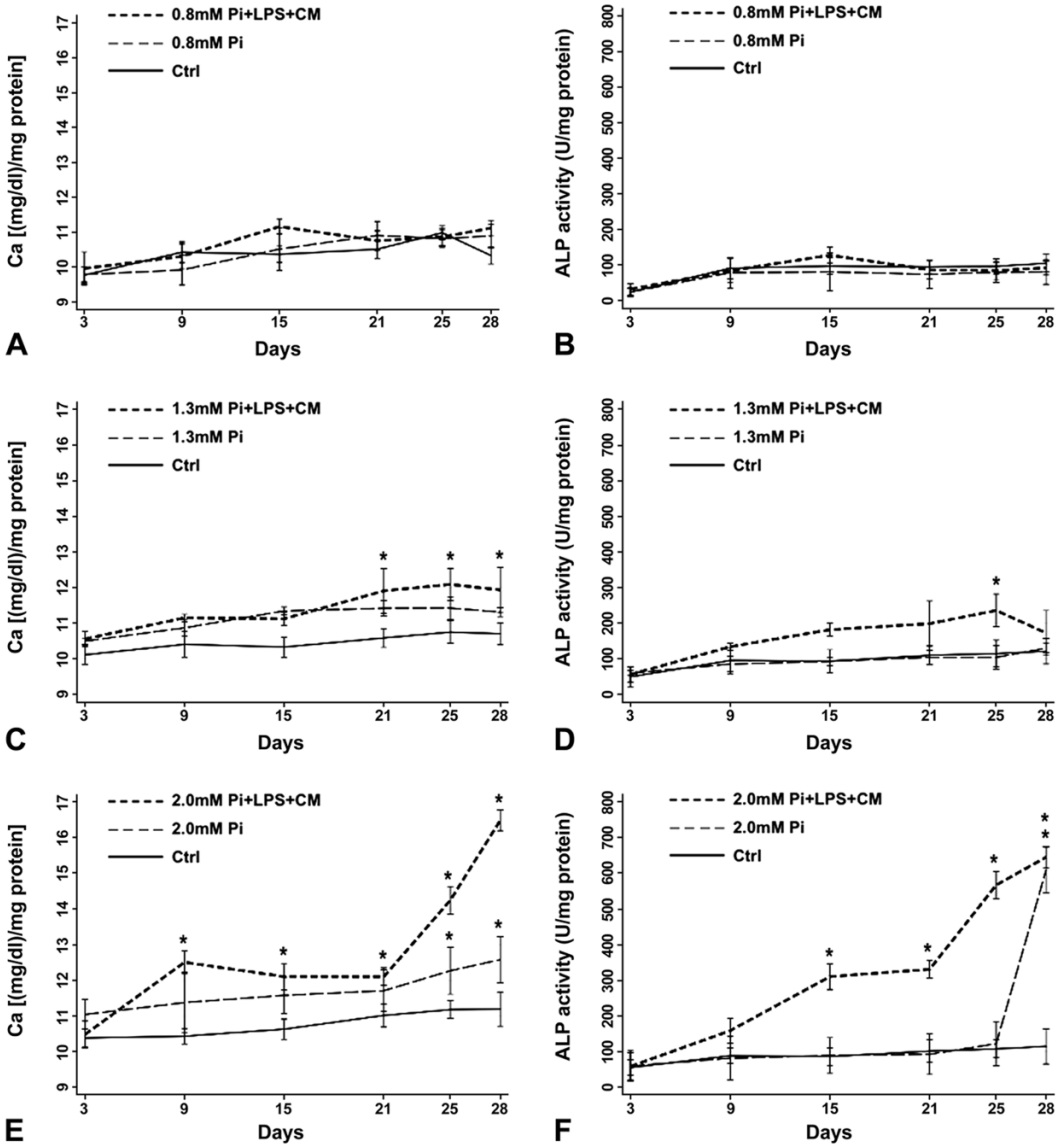

Figure 1. Spectrophotometric quantification of calcium amounts and alkaline phosphatase activity. Calcium content (left column) and enzymatic activity (right column) in 3- to 28-day-long (A–F) control AVICs and AVICs treated with (A, B) 0.8-mM Pi, (C, D) 1.3-mM Pi, and (E, F) 2.0-mM Pi solely or superstimulated with LPS and CM derived from LPS-stimulated macrophages. Values are reported as mean ± SD. Statistically significant values are indicated with asterisks. Abbreviations: AVIC, aortic valve interstitial cell; Pi, phosphate; LPS, lipopolysaccharide; CM, conditioned medium.

Mann–Whitney test, as appropriate. Comparisons between incubation times within each group were achieved using the paired *t*-test or Wilcoxon signed-rank test. Bonferroni correction for multiple comparisons was applied.

Results

Spectrophotometric Quantifications

Spectrophotometric analyses indicated that calcium amounts and ALP activity associate with Pi concentrations and incubation times, with both parameters being enhanced by additional proinflammatory stimuli to various degrees. In more detail, there was slight time-dependent increase in both calcium amounts (Fig. 1A) and ALP activity (Fig. 1B) for 0.8-Pi-cultures and 0.8-Pi-LPS-CM-cultures, with the same trend resulting for control-cultures. Additional slight calcium increases resulted for 1.3-Pi-cultures and 1.3-Pi-LPS-CM-cultures, with these latter showing more significant increase starting from day 21 (Fig. 1C). Concerning ALP activity, evident increase was restricted to 1.3-Pi-LPS-CM-cultures (Fig. 1D). Also, 2.0-Pi-cultures showed slight time-dependent mineral increases, which were more marked starting from day 25. Conversely, sudden

increases in calcium amounts resulted for 2.0-Pi-LPS-CM-cultures, which underwent further striking increase starting from day 21 (Fig. 1E). Sudden, even more marked increases in ALP activity characterized 2.0-Pi-LPS-CM-cultures again, whereas enzyme activity remained at stable levels in 2.0-Pi-cultures, except for its dramatic surge starting from day 25 (Fig. 1F).

Light and Electron Microscopy

Under the inverted microscope, in contrast with control-cultures (not shown), 0.8-Pi-cultures, 0.8-Pi-LPS-CM-cultures, 1.3-Pi-cultures, and 1.3-Pi-LPS-CM-cultures (Fig. 2A–D), calcific nodules appeared for 2.0-Pi-cultures and, at greater extent, 2.0-Pi-LPS-CM-cultures starting from day 21 (Fig. 2E and F). Ultrastructurally, control AVICs exhibited well-preserved organelles including a lot of autophagic vacuoles as usually shown by cultured cells (Fig. 3A and B). Compared with controls, AVICs from 0.8-Pi-cultures and 1.3-Pi-cultures showed mild time-dependent changes, whereas those from 0.8-Pi-LPS-CM-cultures and 1.3-Pi-LPS-CM-cultures underwent an evident appearance of hypertrophic rough endoplasmic reticulum (RER) enclosing distinct cytoplasm regions containing mitochondria and preexistent autophagosomes (Fig. 3C). Further time-dependent RER swelling resulted in a lot of narrow cytoplasm compartments enveloping degenerating mitochondria, disrupting autophagosomes, and remnants of other cytoplasmic components (Figs. 3D and 4A, C). Positivity for acid phosphatase activity resulted at the level of lumens of enlarging RER, its membranes, and enveloped mitochondria (Fig. 4B and D). In contrast, AVICs from 2.0-Pi-cultures and above all those from 2.0-Pi-LPS-CM-cultures appeared to have undergone more and more severe alterations consisting in (1) marked decrease in autophagic vacuoles in the absence of apparent RER hypertrophy; (2) swelling of intracytoplasmic organelles with dissolution of their membranes paralleled by appearance of lipid droplets showing acidification, as revealed by increasing reactivity to preembedding CB reaction (Fig. $5A_1$), and calcium binding capacity, as revealed by postembedding von Kossa silver staining (Fig. $5A_2$); (3) progressive lipid droplet melting with concurrent intracytoplasmic accumulation of phthalocyanine-positive and silver-reactive amorphous material (PPM; Fig. $5A_2$); (4) PPM layering at cell edges so forming PPLs (Fig. $5B_1$), showing enhanced affinity for metallic silver deposition after von Kossa reaction (Fig. $5B_2$) and representing initial HA crystal nucleation foci (Fig. 5C); and (5) AVIC fragmentation into irregularly shaped and sized products lined by concentric PPLs in their turn stemming paracrystalline PPL-lined calcospherulae with persistent reactivity to CB and HA nucleation capacity (Fig. 5D, E_1, and E_2). Of interest, early degenerative patterns characterizing most AVICs from 2.0-Pi-LPS-CM-cultures, such as lipid droplet accumulation and PPM formation, were occasionally found also in AVICs from 1.3-Pi-LPS-CM-cultures (not shown).

Immunocytochemical and Immunoblot Assays

To explore whether the AVIC responses described above may correlate with macroautophagocytosis occurrence, immunocytochemical assays of marker MAP1LC3 were performed. Marked reactivity was restricted to 3-day-long control-cultures and 1.3-Pi-LPS-CM-cultures, with a drastic decrease after longer incubation times (not shown). Percentages of immunopositive cells are displayed in Fig. 6A. To assess possible involvement of apoptosis in driving AVIC responses, immunocytochemical detection of late marker annexin-V was carried out. Negligible reactivity resulted for all cultures irrespective of incubation times (not shown). Percentages of immunopositive cells are displayed in Fig. 6B. In addition, immunoblot assays revealed a complete absence of the 17-kDa caspase-3 cleaved form for all cultures (data not shown). Moreover, ultrastructural examination of 2.0-Pi-LPS-CM-cultures treated with pancaspase inhibitor Boc-D-FMK showed AVICs to undergo degenerative patterns as those observed for AVICs from 2.0-Pi-LPS-CM-cultures not subjected to caspase inhibition (not shown).

Discussion

In the present investigation, possibility of different Pi-concentration-dependent cell responses to be induced was tested in vitro treating AVICs with three Pi concentrations within the normal range in organisms which included maximum and minimum threshold values. Two distinct cell fates, consisting in autophagy-related survival versus procalcific death, resulted to depend on Pi concentration, with possible enhancement caused by additional proinflammatory mediators. Namely, an atypical autophagic activity characterized by an RER-dependent organelle segregation and digestion took place in AVICs cultured at 0.8- and 1.3-mM Pi. Conversely, a peculiar lipid-release-associated procalcific death occurred in AVICs cultured at 2.0-mM Pi, according to the cell degenerative patterns previously described for bovine AVICs cultured under severe dystrophic- and metastatic-like conditions[22,23] as well as porcine AVICs populating aortic valve leaflets subjected to

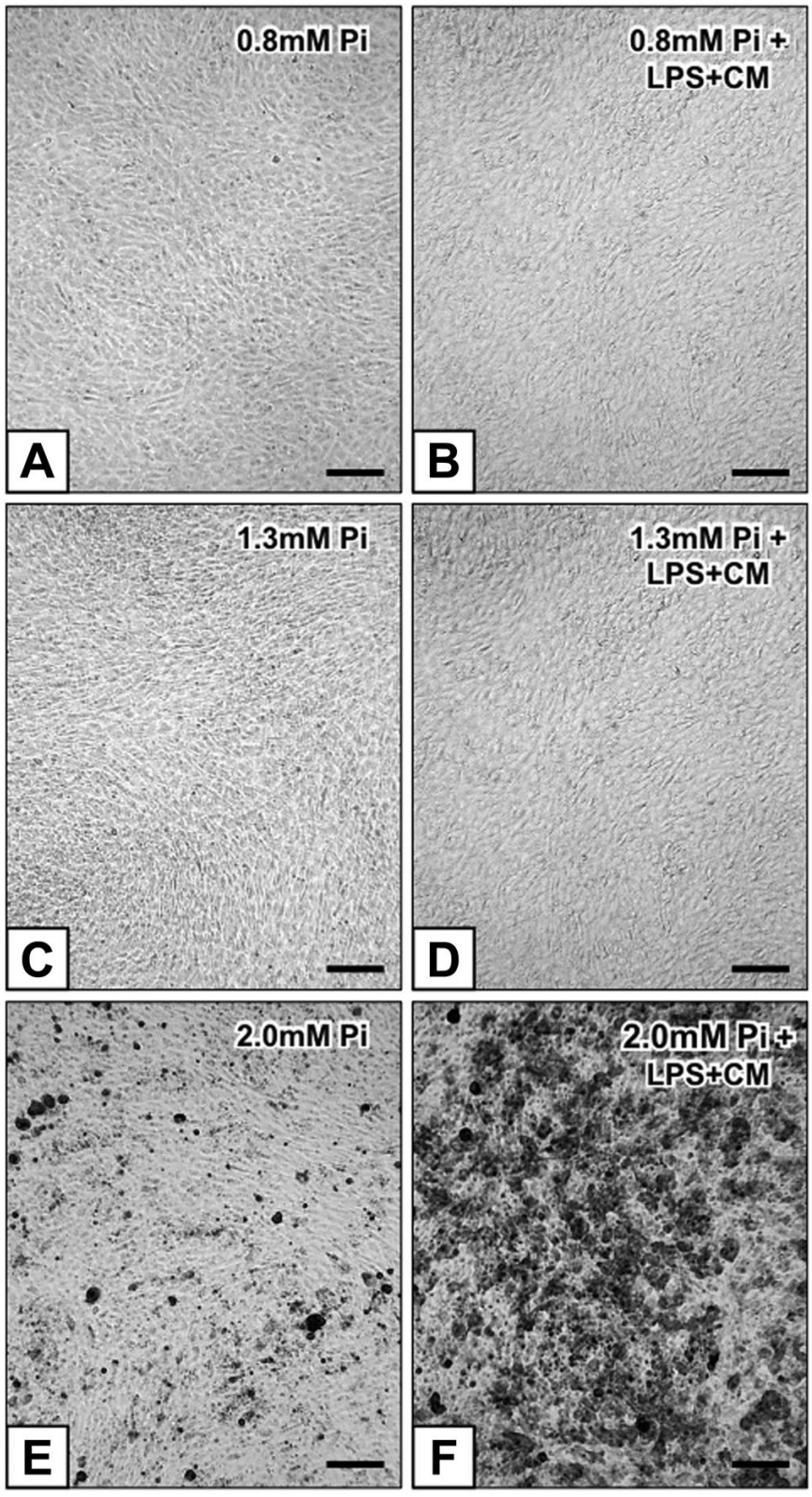

Figure 2. Inverted microscope micrographs of 21-day-long AVIC cultures subjected to alizarin red S calcium staining: (A) unreacted 0.8-Pi-cultures, (B) 0.8-Pi-LPS-CM-cultures, (C) 1.3-Pi-cultures, (D) 1.3-Pi-LPS-CM-cultures, (E) calcium precipitation in 2.0-Pi-cultures, and (F) its increase in 2.0-Pi-LPS-CM-cultures. Abbreviations: AVIC, aortic valve interstitial cell; Pi, phosphate; LPS, lipopolysaccharide; CM, conditioned medium. Scale bars: A–F = 100 μm.

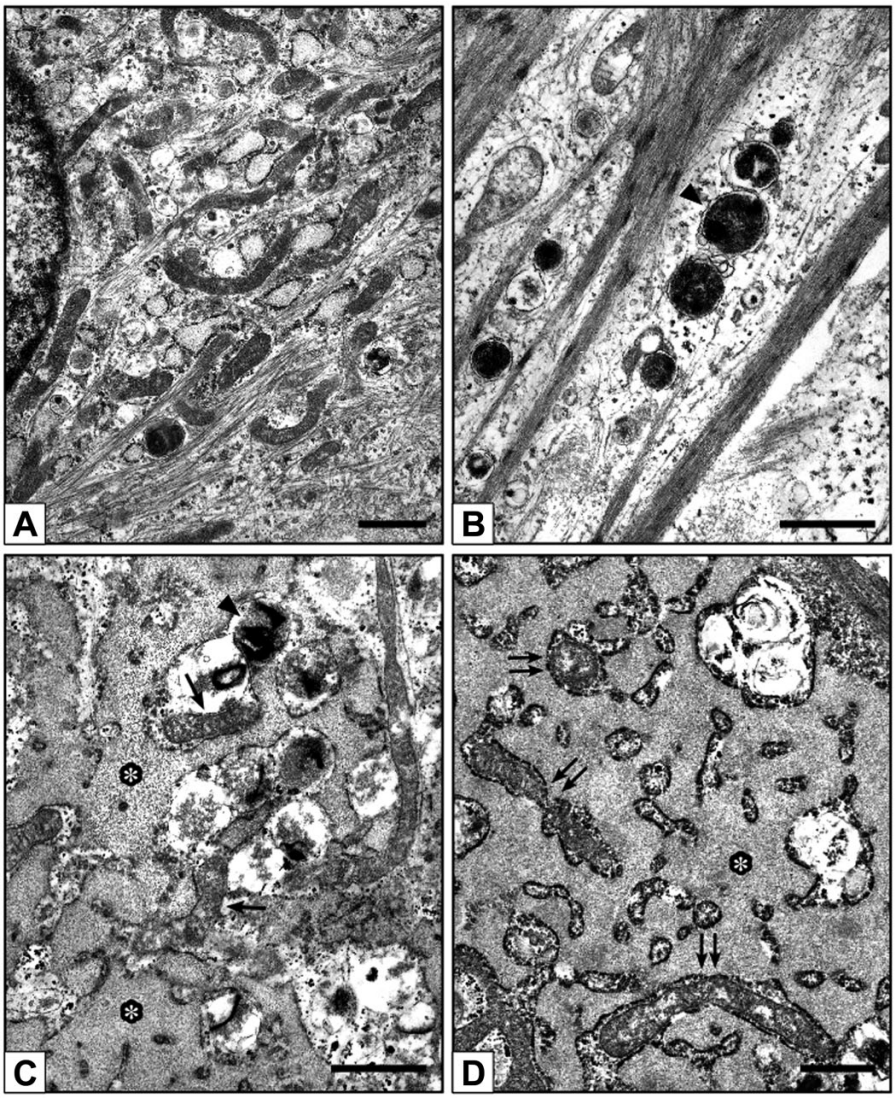

Figure 3. Electron microscope micrographs of 21-day-long AVIC cultures. (A, B) Control AVICs showing normal features including abundant autophagic vacuoles (arrowhead in B). (C, D) AVICs from 0.8-Pi-LPS-CM-cultures showing an abnormal enlargement of the rough endoplasmic reticulum (asterisks), enveloping mitochondria (arrows in C and double arrows in D), autophagosomes (arrowhead in C), and other degrading cytoplasmic components. Abbreviations: AVIC, aortic valve interstitial cell; Pi, phosphate; LPS, lipopolysaccharide; CM, conditioned medium. Scale bars: A–D = 1 μm.

xenogeneic subdermal implantation.[24–27] Consistently, observational studies reported an increased risk of cardiovascular diseases including calcific events in individuals with serum Pi levels just below the upper limit of the conventional normophosphatemic range.[2,3,6–8] Moreover, 1.3-mM Pi concentration representing a critical threshold for augmented valve disease risk[2,6,7] was here supported by the finding that some AVICs from 1.3-Pi-LPS-CM-cultures underwent initial procalcific degeneration, suggesting that such a Pi level can actually be permissive of cell mineralization to some extent. However, notable cell procalcific degeneration was restricted to AVIC cultures containing 2.0-mM Pi for which spectrophotometric analyses revealed linear increases in calcium amounts starting from day 21, consistently with appearance of alizarin-red-S-positive calcific nodules and von-Kossa-positive cell-derived products acting as major HA nucleators, with these latter mirroring those reported for actual aortic valve calcification[28–32] as well as in vivo and in vitro procalcific conditions.[22–27] Additional increases in calcium amounts and ALP activity were observed for AVICs superstimulated with CM from LPS-stimulated macrophages plus LPS in the presence of 2.0-mM Pi. This effect may depend on simultaneous AVIC stimulation by proinflammatory mediators

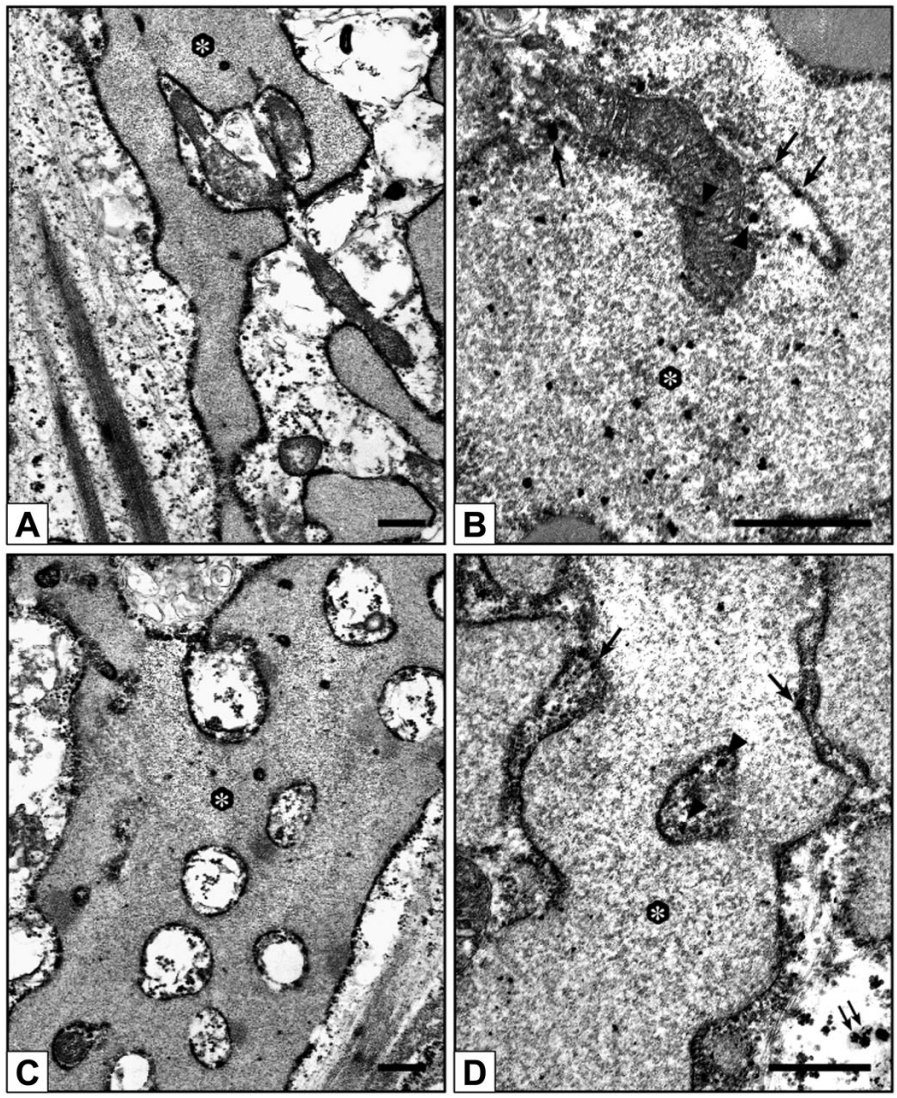

Figure 4. Electron microscope micrographs of 21-day-long 1.3-Pi-LPS-CM-cultures. (A, C) AVICs showing prominent segregation of cytoplasm components by hypertrophic rough endoplasmic reticulum (asterisks). (B, D) AVICs from parallel 1.3-Pi-LPS-CM-cultures showing positivity to acid phosphatase activity as revealed by lead precipitation at the level of reticulum lumen (asterisks) and membrane (arrows in B and D) as well as entrapped organelles (arrowheads in B and D) and organelle remnants (double arrows in D). Abbreviations: Pi, phosphate; LPS, lipopolysaccharide; CM, conditioned medium; AVIC, aortic valve interstitial cell. Scale bars: A–D = 0.5 μm.

contained in the CM[33] and LPS, with this latter possibly causing ALP activity enhancement and concurrent removal of mineralization inhibitor pyrophosphate as reported for cultured human AVICs.[34–36] Because such inflammation-dependent mineralization enhancement was restricted to AVIC cultures containing 2.0-mM Pi, proinflammatory mediators seem to act as stimuli exacerbating the Pi-dependent calcific effects rather than procalcific factors per se. Indeed, as we previously reported,[23] cell mineralization does not occur in AVIC cultures free from elevated Pi supplementation. Accordingly, the drastic increase in ALP activity occurring at day 25 also for LPS-free 2.0-Pi-cultures supports the idea that Pi concentration is the crucial factor involved in cell mineralization.[4,9,10] Even if ALP activity increase was often reported to be associated with the expression of an osteoblast phenotype by mineralizing AVICs,[13,37,38] in the present study, no cell osteoblastic transdifferentiation was ultrastructurally found but only the peculiar AVIC procalcific degeneration and death described. These degenerative features are superimposable to those already reported for cultured AVICs in experimental dystrophic- and metastatic-like calcific conditions,[22,23]

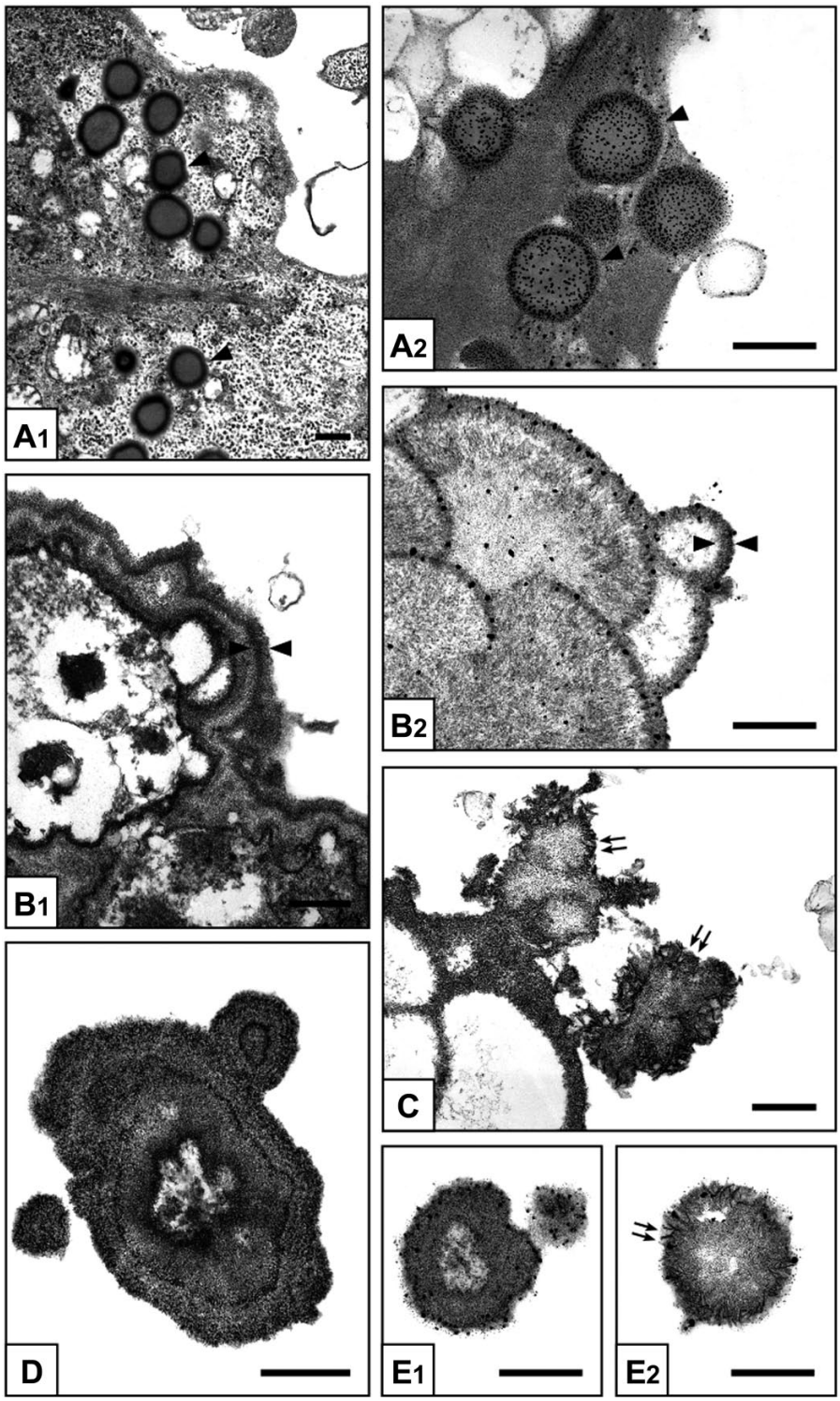

Figure 5. Electron microscope micrographs of 3- to 28-day-long 2.0-Pi-LPS-CM-cultures. AVICs show progressive procalcific degenerative patterns consisting in (A_1) intracellular accumulation of lipid droplets (arrowheads), (A_2) which are positive for von Kossa silver staining (arrowheads); (B_1) margination of released lipids forming CB-positive layers at cell edges (counterposed arrowheads), (B_2) which are sites of silver particle deposition after von Kossa reaction (counterposed arrowheads) and (C) HA crystal nucleation (double arrows); and (D) cell disruption into irregularly shaped cell-derived products, stemming (E_1) small calcospherulae preserving positivity to von Kossa reaction and (E_2) HA nucleation capacity (double arrows). Abbreviations: Pi, phosphate; LPS, lipopolysaccharide; CM, conditioned medium; AVIC, aortic valve interstitial cell; CB, Cuprolinic Blue; HA, hydroxyapatite. Scale bars: A, $B_{1,2}$, C, D, $E_{1,2}$ = 0.5 µm.

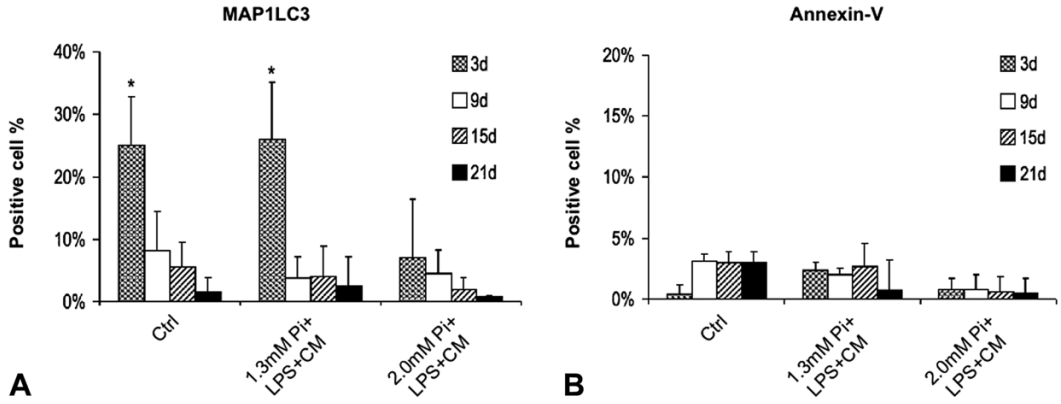

Figure 6. Percentage value histograms. (A) Percentage of AVICs immunopositive for mature autophagosome marker MAP1LC3 and (B) late apoptosis marker annexin-V in 3- to 21-day-long control-cultures, 1.3-Pi-LPS-CM-cultures, and 2.0-Pi-LPS-CM-cultures. Values are reported as mean ± SD. Statistically significant values are indicated with asterisks. Abbreviations: AVIC, aortic valve interstitial cell; Pi, phosphate; LPS, lipopolysaccharide; CM, conditioned medium.

as well as in subdermally implanted aortic valve leaflets,[24–27] according to a process which is more consistent with the concept that ectopic mineralization occurs independently of AVIC osteoblastic differentiation and subsequent bone neogenesis. This result does not call into question whether ossification can take place in calcifying valves,[12,13,16] but the concept is supported that AVIC mineralization is not necessarily related to this histogenetic process.[11] As a matter of fact, bone metaplasia was reported to be histologically recognizable in less than 13% of hundreds of aortic valves affected by dystrophic calcification.[13,39] Although AVIC mineralization is reported to be restricted to specific cell subtypes,[40–42] the choice to use the complete AVIC population was made with the rationale to better reproduce actual in vivo conditions, including cell-to-cell interactions. In mineralizing AVICs, the CB reactivity and von Kossa positivity observed starting from the periphery of the early new-formed lipid droplets may correlate with initial outer lipid acidification,[24,25] with this chemical change likely depending on oxidative effects exerted by endogenous reactive oxygen species (ROS) released by degenerating mitochondria,[43] possibly reinforced by additional macrophage-derived ROS contained in the CM.[44] Such oxidizing environment may also cause phospholipid disarray of lysosome membranes, with release of acid hydrolases, as well as mitochondrial and RER membranes, with calcium leakage and activation of intracellular calcium-dependent enzymes, enabling the occurrence of the autolytic colliquative process observed for mineralizing AVICs, besides causing cytoskeleton disintegration[45] with plasma membrane blebbing and pinching off of multiple procalcific cell by-products. In addition, cell exposure to oxidative stress was reported to contribute to RER stress, leading to the activation of the signaling pathway called unfolded protein response (UPR).[46,47] Taking into account that UPR execution requires RER expansion,[48] the unusually RER oversizing observed for 0.8-Pi-LPS-CM-cultures and 1.3-Pi-LPS-CM-cultures might depend on toxic effects exerted by oxidative stress together with low Pi concentrations, with triggering of transient compensatory mechanisms by cells. Consistently, replacement of stimulating media with standard culture medium was associated with disappearance of RER hypertrophy for these AVIC cultures (unpresented data). As hypertrophic RER was found to segregate damaged mitochondria into more and more narrow compartments, it is likely that their sequestration may ensure prompt buffering of increasing intracytoplasmic calcium via its direct uptake into RER cisternae. This relationship is consistent with the occurrence of direct communication between mitochondrial intermembrane space and RER lumen at the level of topical contact sites, as reported.[49,50] On the contrary, the seemingly unaltered mitochondria entrapped by the hypertrophic RER might uptake calcium from RER cisternae reinforcing their bioenergetic response and improving cell adaptation to stressing conditions.[51] Conversely, the occasional identification of RER hypertrophy in mineralizing AVICs suggests that elevated Pi concentrations may lead to cell death because of excessive intoxication compromising the activation of compensatory responses by the stressed cells. Of note, the ultracytochemical identification of acid phosphatase activity at the level of membranes and lumen of the hypertrophic RER strongly suggests its involvement in an alternative, non-lysosomal mechanism of organelle digestion taking place in AVICs cultured under low/middle Pi

concentrations, as shown for other cells using the same approach.[52–54] As autophagosomes themselves appeared to be removed by such RER-associated degrading activity, this atypical autophagocytosis may somehow represent a time-saving process providing faster recovery of homeostatic conditions by stressed cells than the activation of orthodox macroautophagocytosis machinery can do. Consistently, sudden decrease in autophagic vacuoles and immunoreactivity to mature autophagosome marker MAP1LC3 were observed, suggesting that macroautophagocytosis is just to be conceived as a constitutive house-keeping process providing adaptive cell responses to the culture environment[55] instead of a procalcific process as reported.[20] RER-associated autophagic activity possibly playing a cell survival role was further supported by the fact that negligible immunopositivity to late apoptosis marker annexin-V as well as a complete absence of the 17-kDa caspase-3 cleaved form resulted for all AVICs cultured under low/middle Pi concentrations. As these results were also shared by AVICs cultured at 2.0-mM Pi, AVIC mineralization can be assumed to take place independently from apoptosis occurrence, despite its widely accepted involvement in cardiovascular tissue mineralization.[17 –19,21] Moreover, apoptotic cascade to be not activated in mineralizing AVICs was supported by the occurrence of lipid-release-associated procalcific cell death also in AVICs from 2.0-Pi-LPS-CM-cultures treated with pancaspase inhibitor Boc-D-FMK, besides the fact that typical apoptosis features, such as cell shrinkage and chromatin condensation/fragmentation, were not ultrastructurally encountered. As main features associated with oncosis, such as chromatin clumping, cytoplasm blebbing, and cellular swelling, were not found too, occurrence of an alternative type of cell death in mineralizing AVICs could be assumed, depending on a distinct process resulting in a lipid-release-associated cell degeneration, as observed in the present procalcific conditions and other valve mineralization processes.[22–27] In conclusion, the present findings suggest that Pi represents a specific cell stressor, the concentration of which is critical for AVIC fate, being elevated Pi concentration the major determinant of a distinct procalcific cell death other than apoptosis or oncosis whereas low/middle Pi concentrations trigger the activation of compensatory mechanisms preserving cell functionality via an unusual RER-dependent autophagic activity. In addition, the concept is supported that distinct serum Pi levels are predictive of dystrophic valve calcification incurrence although they are comprised within the conventional normophosphatemic range, suggesting that more meticulous statement of Pi threshold values in organisms is mandatory to properly evaluate the risk of this valve disorder.

Acknowledgment

The authors thank Dr. Emanuela Tesei, official veterinarian of Pitaccolo slaughterhouse, for her kind support in providing the animal tissues used in the present study.

Competing Interests

The author(s) declared no potential conflicts of interest with respect to the research, authorship, and/or publication of this article.

Author Contributions

AB: manuscript writing, contribution in designing this study, ultracytochemical and immunocytochemical reactions, and ultrastructural analyses; ADM: cell extraction, culturing, and treatments, and Western blot analyses; MC: image processing and panel preparation; GG: statistical analyses; FT: spectrophotometric analyses and data elaboration; MM: manuscript revision; and FO: design and supervision of this investigation, and manuscript revision.

Funding

The author(s) received no financial support for the research, authorship, and/or publication of this article.

Literature Cited

1. Nkomo VT, Gardin JM, Skelton TN, Gottdiener JS, Scott CG, Enriquez-Sarano M. Burden of valvular heart diseases: a population-based study. Lancet. 2006;368:1005–11.
2. Tonelli M, Sacks F, Pfeffer M, Gao Z, Curhan G. Relation between serum phosphate level and cardiovascular event rate in people with coronary disease. Circulation. 2005;112:2627–33.
3. Osuka S, Razzaque MS. Can features of phosphate toxicity appear in normophosphatemia? J Bone Miner Metab. 2012;30:10–8.
4. Jono S, McKee MD, Murry CE, Shioi A, Nishizawa Y, Mori K, Morii H, Giachelli CM. Phosphate regulation of vascular smooth muscle cell calcification. Circ Res. 2000;87:E10–7.
5. Rodriguez-Benot A, Martin-Malo A, Alvarez-Lara A, Rodriguez M, Aljama P. Mild hyperphosphatemia and mortality in hemodialysis patients. Am J Kidney Dis. 2005;46:68–77.
6. Foley RN. Phosphate levels and cardiovascular disease in the general population. Clin J Am Soc Nephrol. 2009;4:1136–9.
7. van Kuijk JP, Flu WJ, Chonchol M, Valentijn TM, Verhagen HJM, Bax JJ, Poldermans D. Elevated preoperative phosphorus levels are an independent risk factor for cardiovascular mortality. Am J Nephrol. 2010;32:163–8.
8. Ellam TJ, Chico TJA. Phosphate: the new cholesterol? the role of the phosphate axis in non-uremic vascular disease. Atherosclerosis. 2012;220:310–8.
9. Kirsch T. Determinants of pathological mineralization. Curr Opin Rheumatol. 2006;18:174–80.

10. Giachelli CM. The emerging role of phosphate in vascular calcification. Kidney Int. 2009;75:890–7.
11. Kim KM. Apoptosis and calcification. Scanning Microsc. 1995;9:1137–78.
12. Mohler ER III, Gannon F, Reynolds C, Zimmerman R, Keane MG, Kaplan FS. Bone formation and inflammation in cardiac valves. Circulation. 2001;103:1522–8.
13. Rajamannan NM, Subramaniam M, Rickard D, Stock SR, Donovan J, Springett M, Orszulak T, Fullerton DA, Tajik AJ, Bonow RO, Spelsberg T. Human aortic valve calcification is associated with an osteoblast phenotype. Circulation. 2003;107:2181–4.
14. Freeman RV, Otto CM. Spectrum of calcific aortic valve disease. Pathogenesis, disease progression, and treatment strategies. Circulation. 2005;111:3316–26.
15. Demer LL, Tintut Y. Inflammatory, metabolic, and genetic mechanisms of vascular calcification. Arterioscler Thromb Vasc Biol. 2014;34:715–23.
16. Yutzey KE, Demer LL, Body SC, Huggins GS, Towler DA, Giachelli CM, Hofmann-Bowman MA, Mortlock DP, Rogers MB, Sadeghi MM, Aikawa E. Calcific aortic valve disease: a consensus summary from the Alliance of Investigators on Calcific Aortic Valve Disease. Arterioscler Thromb Vasc Biol. 2014;34:2387–93.
17. Lee YS, Chou YY. Pathogenetic mechanism of senile calcific aortic stenosis: the role of apoptosis. Chin Med J (Engl). 1998;111:934–9.
18. Proudfoot D, Skepper JN, Hegyi L, Bennett MR, Shanahan CM, Wiessberg PL. Apoptosis regulates human vascular calcification in vitro: evidence for initiation of vascular calcification by apoptotic bodies. Circ Res. 2000;87:1055–62.
19. Jian B, Narula N, Li QY, Mohler ER, Levy RJ. Progression of aortic valve stenosis: TGF-beta1 is present in calcified aortic valve cusps and promotes aortic valve interstitial cell calcification via apoptosis. Ann Thorac Surg. 2003;75:457–66.
20. Somers P, Knaapen M, Kockx M, van Cauwelaert P, Bortier H, Mistiaen W. Histological evaluation of autophagic cell death in calcified aortic valve stenosis. J Heart Valve Dis. 2006;15:43–8.
21. Clarke MCH, Littlewood TD, Figg N, Maguire JJ, Davenport AP, Goddard M, Bennett MR. Chronic apoptosis of vascular smooth muscle cells accelerates atherosclerosis and promotes calcification and medial degeneration. Circ Res. 2008;102:1529–38.
22. Ortolani F, Rigonat L, Bonetti A, Contin M, Tubaro F, Rattazzi M, Marchini M. Pro-calcific responses by aortic valve interstitial cells in a novel in vitro model simulating dystrophic calcification. Ital J Anat Embryol. 2010;115:135–9.
23. Bonetti A, Della Mora A, Contin M, Tubaro F, Marchini M, Ortolani F. Ultrastructural and spectrophotometric study on the effects of putative triggers on aortic valve interstitial cells in in vitro models simulating metastatic calcification. Anat Rec. 2012;295:1117–27.
24. Ortolani F, Petrelli L, Tubaro F, Spina M, Marchini M. Novel ultrastructural features as revealed by phthalocyanine reactions indicate cell priming for calcification in subdermally implanted aortic valves. Connect Tissue Res. 2002;43:44–55.
25. Ortolani F, Tubaro F, Petrelli L, Gandaglia A, Spina M, Marchini M. Copper retention, calcium release and ultrastructural evidence indicate specific Cuprolinic Blue uptake and peculiar modifications in mineralizing aortic valves. Histochem J. 2002;34:41–50.
26. Ortolani F, Petrelli L, Nori SL, Spina M, Marchini M. Malachite green and phthalocyanine-silver reactions reveal acidic phospholipid involvement in calcification of porcine aortic valves in rat subdermal model. Histol Histopathol. 2003;18:1131–40.
27. Ortolani F, Bonetti A, Tubaro F, Petrelli L, Contin M, Nori SL, Spina M, Marchini M. Ultrastructural characterization of calcification onset and progression in subdermally implanted aortic valves. Histochemical and spectrometric data. Histol Histopathol. 2007;22:261–72.
28. Kim KM, Huang S. Ultrastructural study of calcification of human aortic valve. Lab Invest. 1971;25:357–66.
29. Kim KM. Calcification of matrix vesicles in human aortic valve and aortic media. Fed Proc. 1976;35:156–62.
30. Boskey AL, Bullough PG, Vigorita V, Di Carlo E. Calcium-acidic phospholipid-phosphate complexes in human hydroxyapatite-containing pathologic deposits. Am J Pathol. 1988;133:22–9.
31. Kim KM, Trump BF. Amorphous calcium precipitates in human aortic valve. Calcif Tissue Res. 1975;18:155–60.
32. Kim KM, Valigorsky JM, Mergner WJ, Jones RT, Pendergrass RF, Trump BF. Aging changes in the human aortic valve in relation to dystrophic calcification. Hum Pathol. 1976;7:47–60.
33. Sweet MJ, Hume DA. Endotoxin signal transduction in macrophages. J Leukoc Biol. 1996;60:8–26.
34. Babu AN, Meng X, Zou N, Yang X, Wang M, Song Y, Cleveland JC, Weyant M, Banerjee A, Fullerton DA. Lipopolysaccharide stimulation of human aortic valve interstitial cells activates inflammation and osteogenesis. Ann Thorac Surg. 2008;86:71–6.
35. Meng X, Ao L, Song Y, Babu A, Yang X, Wang M, Weyant MJ, Dinarello CA, Cleveland JC Jr, Fullerton DA. Expression of functional Toll-like receptors 2 and 4 in human aortic valve interstitial cells: potential roles in aortic valve inflammation and stenosis. Am J Physiol Cell Physiol. 2008;294:C29–35.
36. Yang X, Fullerton DA, Su X, Ao L, Cleveland JC Jr, Meng X. Pro-osteogenic phenotype of human aortic valve interstitial cells is associated with higher levels of toll-like receptors 2 and 4 and enhanced expression of bone morphogenetic protein 2. J Am Coll Cardiol. 2009;53:491–500.
37. Mathieu P, Voisine P, Pépin A, Shetty R, Savard N, Dagenais F. Calcification of human valve interstitial cells is dependent on alkaline phosphatase activity. J Heart Valve Dis. 2005;14:353–7.
38. Feng X, Li JM, Liao XB, Hu YR, Shang BP, Zhang ZY, Yuan LQ, Xie H, Sheng ZF, Tang H, Zhang W, Gu L, Zhou XM. Taurine suppresses osteoblastic differentiation of aortic valve interstitial cells induced by beta-glycerophosphate disodium, dexamethasone and

ascorbic acid via the ERK pathway. Amino Acids. 2012;43: 1697–704.
39. Steiner I, Kasparová P, Kohout A, Dominik J. Bone formation in cardiac valves: a histopathological study of 128 cases. Virchows Arch. 2007;450:653–7.
40. Mohler ER III, Chawla MK, Chang AW, Vyavahare N, Levy RJ, Graham L, Gannon FH. Identification and characterization of calcifying valve cells from human and canine aortic valves. J Heart Valve Dis. 1999;8:254–60.
41. Rattazzi M, Iop L, Faggin E, Bertacco E, Zoppellaro G, Baesso I, Puato M, Torregrossa G, Fadini GP, Agostini C, Gerosa G, Sartore S, Pauletto P. Clones of interstitial cells from bovine aortic valve exhibit different calcifying potential when exposed to endotoxin and phosphate. Arterioscler Thromb Vasc Biol. 2008;28:2165–72.
42. Masjedi S, Amarnath A, Baily KM, Ferdous Z. Comparison of calcification potential of valvular interstitial cells isolated from individual aortic valve cusps. Cardiovasc Pathol. 2016;25:185–94.
43. Li X, Fang P, Mai J, Choi ET, Wang H, Yang XF. Targeting mitochondrial reactive oxygen species as novel therapy for inflammatory diseases and cancers. J Hematol Oncol. 2013;6:19.
44. Wu TT, Chen TL, Chen RM. Lipopolysaccharide triggers macrophage activation of inflammatory cytokine expression, chemotaxis, phagocytosis, and oxidative ability via a toll-like receptor 4-dependent pathway: validated by RNA interference. Toxicol Lett. 2009;191:195–202.
45. Smith MW, Phelps PC, Trump BF. Cytosolic Ca^{2+} deregulation and blebbing after $HgCl_2$ injury to cultured rabbit proximal tubule cells as determined by digital imaging microscopy. Proc Natl Acad Sci U S A. 1991;88:4926–30.
46. Malhotra JD, Kaufman RJ. Endoplasmic reticulum stress and oxidative stress: a vicious cycle or a double-edged sword? Antioxid Redox Signal. 2007;9:2277–93.
47. Malhotra JD, Miao H, Zhang K, Wolfson A, Pennathur S, Pipe SW, Kaufman RJ. Antioxidants reduce endoplasmic reticulum stress and improve protein secretion. Proc Natl Acad Sci U S A. 2008;105:18525–30.
48. Schröder M. Endoplasmic reticulum stress responses. Cell Mol Life Sci. 2008;65:862–94.
49. de Brito OM, Scorrano L. Mitofusin 2 tethers endoplasmic reticulum to mitochondria. Nature. 2008;456:605–10.
50. Giorgi C, De Stefani D, Bononi A, Rizzuto R, Pinton P. Structural and functional link between the mitochondrial network and the endoplasmic reticulum. Int J Biochem Cell Biol. 2009;41:1817–27.
51. Bravo R, Vicencio JM, Parra V, Troncoso R, Munoz JP, Bui M, Quiroga C, Rodriguez AE, Verdejo HE, Ferreira J, Iglewski M, Chiong M, Simmen T, Zorzano A, Hill JA, Rothermel BA, Szabadkai G, Lavandero S. Increased ER-mitochondrial coupling promotes mitochondrial respiration and bioenergetics during early phases of ER stress. J Cell Sci. 2011;124:2143–52.
52. Borgers M, Thoné F. Further characterization of phosphatase activities using non-specific substrates. Histochem J. 1976;8:301–7.
53. Griffiths GW. Transport of glial cell acid phosphatase by endoplasmic reticulum into damaged axons. J Cell Sci. 1979;36:361–89.
54. Noda T, Farquhar MG. A non-autophagic pathway for diversion of ER secretory proteins to lysosomes. J Cell Biol. 1992;119:85–97.
55. Mizushima N. The pleiotropic role of autophagy: from protein metabolism to bactericide. Cell Death Differ. 2005;12:1535–41.